RESEARCH ARTICLE

Pallidal Gap Junctions-Triggers of Synchrony in Parkinson's Disease?

Bettina C. Schwab,[1,2*] Tjitske Heida,[2] Yan Zhao,[2] Stephan A. van Gils,[1] and Richard J. A. van Wezel[2,3]

[1]*Applied Analysis, MIRA Institute of Technical Medicine and Biomedical Technology, University of Twente, Enschede, The Netherlands*
[2]*Biomedical Signals and Systems, MIRA Institute of Technical Medicine and Biomedical Technology, University of Twente, Enschede, The Netherlands*
[3]*Biophysics, Donders Institute for Brain, Cognition and Behavior, Radboud University, Nijmegen, The Netherlands*

ABSTRACT: Although increased synchrony of the neural activity in the basal ganglia may underlie the motor deficiencies exhibited in Parkinson's disease (PD), how this synchrony arises, propagates through the basal ganglia, and changes under dopamine replacement remains unknown. Gap junctions could play a major role in modifying this synchrony, because they show functional plasticity under the influence of dopamine and after neural injury. In this study, confocal imaging was used to detect connexin-36, the major neural gap junction protein, in postmortem tissues of PD patients and control subjects in the putamen, subthalamic nucleus (STN), and external and internal globus pallidus (GPe and GPi, respectively). Moreover, we quantified how gap junctions affect synchrony in an existing computational model of the basal ganglia. We detected connexin-36 in the human putamen, GPe, and GPi, but not in the STN. Furthermore, we found that the number of connexin-36 spots in PD tissues increased by 50% in the putamen, 43% in the GPe, and 109% in the GPi compared with controls. In the computational model, gap junctions in the GPe and GPi strongly influenced synchrony. The basal ganglia became especially susceptible to synchronize with input from the cortex when gap junctions were numerous and high in conductance. In conclusion, connexin-36 expression in the human GPe and GPi suggests that gap junctional coupling exists within these nuclei. In PD, neural injury and dopamine depletion could increase this coupling. Therefore, we propose that gap junctions act as a powerful modulator of synchrony in the basal ganglia. © 2014 International Parkinson and Movement Disorder Society

Key Words: Connexin-36; oscillations; globus pallidus; confocal microscopy

In patients with Parkinson's disease (PD) and corresponding animal models, unusually high amounts of synchrony, bursting, and low-frequency oscillations have been recorded.[1] These abnormalities are thought to underlie the motor symptoms of PD, but whether they are causal remains unclear.[2] Still, the mechanisms for the emergence and transmission of synchrony and oscillations in the basal ganglia remain debated. Experimental and computational studies have shown that interactions between the subthalamic nucleus (STN) and the external segment of the globus pallidus (GPe) are important for the emergence of synchrony.[3-6] Other studies highlighted the role of synaptic input from the cortex to the STN.[7-11] Changes in the intrinsic properties of the GPe can also lead to synchrony.[12-15] Whereas the healthy GPe shows almost no correlations between pairs of neurons despite the presence of local axon collaterals and correlated inputs,[16,17] synchronization in the β frequency band (13-30 Hz) is prominent after dopamine loss.[16,18,19] Therefore, a decorrelation mechanism has been suggested to exist in the healthy GPe.[17] Given the pacemaking function of GPe neurons, intra-GPe synaptic coupling may play an important role in synchronization and

*Correspondence to: Bettina C. Schwab, Applied Analysis, Department of Applied Mathematics, University of Twente, PO Box 217, 7500 AE Enschede, The Netherlands. Telephone: 0031640177295. E-Mail: b.c.schwab@utwente.nl

Funding agencies: We acknowledge funding of the Netherlands Organization for Scientific Research (NWO) on the NDNS+-project "Desynchronization of Parkinsonian Oscillations in the Subthalamic Nucleus" and from MIRA, Institute for Biomedical Technology and Technical Medicine, University of Twente.

Relevant conflicts of interest/financial disclosures: B. C. Schwab receives funding of the Netherlands Organisation for Scientific Research (NWO) on the NDNS+-project "Desynchronization of Parkinsonian Oscillations in the Subthalamic Nucleus" and from MIRA, Institute for Biomedical Technology and Technical Medicine, University of Twente. She receives human tissue from the Netherlands Brain Bank and is supported by the German National Academic Foundation.

Full financial disclosures and author roles may be found in the online version of this article.

Received: 25 October 2013; **Revised:** 30 June 2014; **Accepted:** 11 July 2014

Published online 13 August 2014 in Wiley Online Library (wileyonlinelibrary.com). DOI: 10.1002/mds.25987

desynchronization in the GPe. However, few experimental studies have described changes in the GPe after dopamine loss that would explain the clear shifts in network dynamics seen in PD. Furthermore, how these mechanisms may change under dopamine replacement remains unclear.

Pallidal gap junctions (GJs) could provide such an intrinsic mechanism of synchronization. Gap junctional coupling (GJC) in cortex and striatum has already been proposed to contribute to the pathology of PD.[20-24] In striatum and cortex, gap junctions between interneurons consist of connexin-36 (Cx36),[25,26] which has also been found in the rat globus pallidus (GP), corresponding to the human GPe.[27] Various other neurological pathologies are thought to involve altered GJC, including epilepsy, stroke, spreading depression, and ischemia.[28-30] All of these pathologies involve neural injury, which is in general associated with remodeling of GJs.[31] Fernandez-Suarez et al.[32] reported the death of parvalbumin-positive γ-aminobutyric acid (GABA)ergic neurons in the GPe of animal models of PD, raising the possibility of GJ remodeling. Dopamine can also influence gap junctional coupling: for example, GJs in the retina change their conductance in response to variations in the dopamine level.[33-35] Most studies on GJs in the brain found a decrease in GJ conductance with increased dopamine levels.[21] Dye coupling, an indication for GJC, was increased in the striatum after dopamine loss in rats.[36,37] Dopamine modulation of GJC in the striatum also has been associated with stereotypic behavior,[38] emphasizing the potential impact of GJC on clinical characteristics. Although the presence of GJs in the human GPe, internal globus pallidus (GPi), and STN would significantly impact information processing in the basal ganglia, whether they exist and how they may remodel after dopamine depletion remains unknown.

We therefore studied Cx36 expression in the putamen, GPe, GPi, and STN of postmortem tissues from PD patients and control subjects. Furthermore, we incorporated GJs into a basic conductance-based computational model of the basal ganglia to examine their potential influence on synchrony. Based on our findings, we hypothesize that GJs exist between GABAergic neurons of the GPe and GPi and suggest that they undergo redistribution because of neural injury in PD and exhibit up-regulated conductances after dopamine depletion. The existence of numerous high-conductance GJs in the GPe may diminish the ability of pallidal neurons to desynchronize correlated input.

Materials and Methods

Human Tissue Preparation

Human tissue was obtained from The Netherlands Brain Bank, Netherlands Institute for Neuroscience, Amsterdam. All material was collected from donors for or from whom written informed consent for a brain autopsy and the use of the material and clinical information for research purposes had been obtained by the Netherlands Brain Bank. One control subject that showed a local bacterial proliferation in the basal ganglia was excluded (not shown in Table 1). All patients were men between 71 and 96 years of age. The control and PD patient groups were matched in age (82 ± 11 years) and postmortem delay (5.1 ± 1.4 h). Based on their clinical information, the control subjects did not suffer from any neurological disease. Quantitative scores on the severity of motor symptoms in the PD patients were not available. The formalin-fixed, paraffin-embedded tissues were deparaffinized using xylene and ethanol. Biopsy specimens were taken from putamen (part of the striatum), GPe, and GPi (6 PD patients and 6 control subjects as described in Table 1) and STN (2 PD patients and 2 control subjects, partly coinciding with the previous group). Tissues were immersed in 25% sucrose for at least 48 hours before being frozen to prevent tissue damage. Frozen biopsy specimens were then sectioned using a cryostat along the coronal plane at a thickness of 60 μm.

Fluorescent Labeling and Confocal Imaging for Cx36 Detection

We used triple labeling to image Cx36 on GABAergic neurons. Free-floating sections were first permeabilized and blocked with phosphate buffered saline containing 0.5% Triton-X-100 and 10% goat serum. Next, sections were incubated in primary and secondary antibodies for approximately 24 hours and 8 hours, respectively. Dilutions (1:300) of mouse monoclonal immunoglobulin IgG1 anti-Cx36 (Invitrogen, Carlsbad, USA) and rabbit polyclonal immunoglobulin IgG anti-GAD-65/67 (Sigma, St. Louis, USA) were used to detect GJs and GABAergic neurons, respectively. 4',6-Diamidino-2-phenylindole was applied in a 1:500 dilution to label the cell nuclei. The secondary antibodies were conjugated to Alexa Fluor 488 and 633 (Invitrogen). To reduce autofluorescence, we applied an autofluorescence eliminator reagent (Millipore, Billerica, USA) for 10 min. The samples were then rinsed in ethanol and mounted on glass slides with Fluoromont-G (Electron Microscopy Sciences, Hatfield, USA). Imaging was performed on a Nikon A1 confocal microscope with a 100× oil lens. To avoid bleed-through, we sequentially scanned the specimens with individual lasers. A minimum of 20 images per tissue group was taken, with a resolution of 1024 × 1024 pixels or 0.124 μm in both directions. Our tissue selection process was not blinded. However, we tried to minimize the effects of unblinded sampling by selecting tissue areas solely based on the 4',6-diamidino-2-phenylindole signal.

TABLE 1. List of patients from whom tissue of putamen, GPe and GPi has been analyzed.

Patient	1	2	3	4	5	6	7	8	9	10	11	12
PD	No	No	No	No	No	No	11 years	8 years	4 years	3 years	21 years	10 years
Cause of death	Heart failure	Bronchus carcinoma	Myocardial infarction	Sepsis	Cardiac asthma	Urinary tract infection	Metabolic de-regulation	Heart failure	Respiratory insufficiency	Respiratory insufficiency	De-hydration	Euthanasia
Age	96	74	87	71	85	96	87	84	83	87	74	81
Post-mortem delay	6 h 30 min	5 h	4 h	7 h 40 min	4 h 15 min	4 h 10 min	4 h 45 min	5 h 10 min	5 h 45 min	7 h 20 min	2 h 50 min	4 h 30 min
Tremor	No	No	No	No	No	No	Yes	Yes	No	Yes	Yes	Yes
Stiffness	No	No	No	No	No	No	Yes	No	Yes	Yes	No	Yes
Brady-/ akinesa	No	No	No	No	No	No	Yes	Yes	Yes	Yes	Yes	Yes
L-Dopa medication	No	No	No	No	No	No	Not during last year	Yes	Yes	Yes	No	Yes
Cx36 Putamen (spots/mm^2)	1770.11	830.06	1266.14	1171.14	1187.16	788.27	2331.67	2158.69	1722.85	865.00	1475.43	1938.93
Cx36 Putamen (spot area/%)	0.02217	0.01780	0.02812	0.01850	0.02625	0.01717	0.03941	0.02427	0.02589	0.01636	0.03772	0.03738
Cx36 GPe (spots/mm^2)	1266.48	902.24	1001.31	370.92	919.42	1082.69	1299.22	1462.38	1579.71	710.65	1254.11	1610.66
Cx36 GPe (spot area/%)	0.01832	0.01339	0.02149	0.00750	0.01881	0.02450	0.02531	0.01658	0.02556	0.01110	0.02942	0.03765
Cx36 GPi (spots/mm^2)	1058.63	556.38	712.29	771.33	709.13	778.60	2165.37	2204.04	1109.00	1954.85	940.23	1219.69
Cx36 GPi (spot area/%)	0.01559	0.00847	0.01307	0.01235	0.01775	0.01539	0.03772	0.02505	0.01718	0.02467	0.02264	0.03335

We show clinical information and detected Cx36 levels for individual subjects and patients. Occurrence of the PD symptoms tremor, stiffness and brady- or akinesia were described based on the clinical reports. The symptoms were assumed to be absent if not mentioned in the report.

Quantification of the Cx36 Signal

Confocal micrographs were analyzed using ImageJ.[39] We used a threshold segmentation approach to quantitatively estimate the level of Cx36 expression: assuming that the image intensity histogram is a bimodal distribution, the threshold was defined as the arithmetic mean of $p1$, the peak intensity of the background noise, and $p2$, the highest signal intensity:

$$t = \frac{(p_1 + p_2)}{2} \tag{1}$$

Images without a bimodal intensity distribution or with bright unspecific staining were rejected. In the segmented image, only spots with an area between 4 and 40 pixels were considered. In this way, segmentation of noise and unspecific labeling was suppressed.

Gap Junctional Coupling in a Basic Model of the Basal Ganglia

Depending on their architecture and strength, GJs can be both synchronizing or desynchronizing[40-42] and can interact in a nonlinear way with inhibitory synapses.[43] Computational modeling can be used to study how a correlated input from cortex to STN affects synchronization, and how synchrony is spread to other nuclei. We implemented the network model proposed by Rubin and Terman,[44] including 16 cells to represent each of STN, GPe, and GPi, using MATLAB.[45] As shown in Figure 1A, the STN received excitatory input from the cortex, and both GPe and GPi received inhibitory input from the striatum. We added GJs between pairs of neurons inside the GPe and GPi. The neural dynamics in the GPe and GPi were thus governed by:

$$C_m \frac{dV}{dt} = -I_{ionic} - I_{syn} - I_{GJ} + I_{app} \tag{2}$$

where C_m is the membrane capacity, V the transmembrane voltage, and I_{ionic}, I_{syn}, I_{GJ}, and I_{app} the ionic, synaptic, GJ, and applied currents, respectively. GJs were modeled as ohmic resistors:

$$I_{GJ} = g_{GJ} \cdot, \Delta V \tag{3}$$

with GJ conductance g_{GJ} . The ΔV represents the difference in transmembrane voltage between the connecting cells. We chose two different GJC architectures (Fig. 1B) to estimate the effect of newly synthesized GJ channels: (1) sparse coupling with an average of 0.5 GJs per cell and (2) numerous coupling with an average of 1 GJ per cell. To simulate dopamine modulation of the GJ strength, the GJ conductance in the GPe (g_{GPe}) and GPi (g_{GPi}) was varied between 0 and 0.25 mS/cm^2, a realistic range for neural GJs[46] but low compared with the conductances of chemical synapses. The STN received excitatory input from the cortex in the form of white noise, either

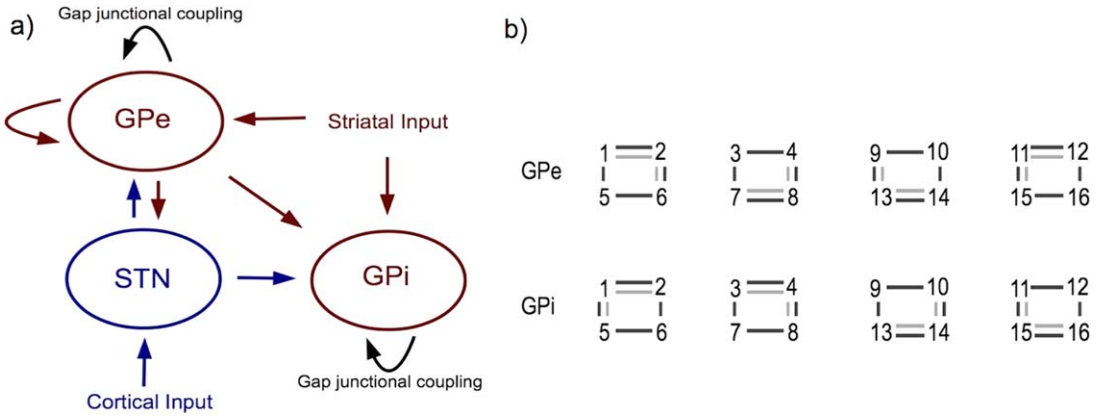

FIG. 1. Placement of GJs added to the Rubin-Terman model [41]. (a) General setup of STN, GPe, GPi and inputs from striatum and cortex. Red indicates inhibitory connections, blue excitatory connections, black GJC. (b) GJ architectures in the GPe and GPi. Numbers represent the 16 cells in both nuclei, connected in groups of four via GJs and in the GPe also via inhibitory synapses (not shown). Light grey lines indicate the architecture for sparse GJC, dark grey lines the architecture for numerous GJC. [Color figure can be viewed in the online issue, which is available at wileyonlinelibrary.com.]

completely correlated or completely uncorrelated. The inhibitory input from the striatum to the GPe and GPi was uncorrelated white noise. To quantify synchrony, we performed principal component analysis on spike activity as described in Lourens.[47] In short, we calculated the number of principal components (PCs) needed to describe 95% of the information contained in the spike times for all 16 cells in each nucleus. High synchronization is associated with a small number of PCs, indicating that little variation is needed to describe the network state.

Results

Cx36 Is Present in the Human Putamen, GPe and GPi, But Not in the STN

The STN tissues from neither PD patients nor control subjects showed significant levels of Cx36 (data not shown) and were thus excluded from further analysis. However, we found a clear punctuate pattern of Cx36 labeling in the putamen, GPe, and GPi of all subjects (Fig. 2), which was absent in a negative control without the primary antibody (data not shown). Table 1 summarizes the clinical background of all subjects and the results of the Cx36 quantification. An average of 18, but at least 12 images per tissue group could be included for image analysis. The GJC in the putamen is well described and thought to be increased after dopamine depletion.[36,37] We therefore used Cx36 expression in the putamen as a reference for numerous GJCs. Control subjects showed the most Cx36 expression in the putamen; less Cx36 was found in their GPe and GPi. Compared with controls, the number of Cx36 spots in PD patients increased by 50% in the putamen, 43% in the GPe and 109% in the GPi (Fig. 3A). Furthermore, the cumulative area of the Cx36 spots increased significantly in the putamen and GPi of PD patients, but no significant increase was detected in the GPe (Fig. 3B).

Gap Junctional Coupling Controls Synchrony in a Basic Model of the Basal Ganglia

Based on our experimental findings of Cx36 in the human GPe and GPi, we used a small network model to demonstrate the effect of GJC in these nuclei. Figure 4 shows the results of our principal component analysis for different GJ densities, GJ conductances g_{GPe} and g_{GPi}, and cortical input. We compared the number of PCs as we increased g_{GPe} and g_{GPe} to model modulation of the GJ conductance by dopamine. For sparse GJC and uncorrelated cortical input, the increase in GJ conductance induced moderate synchronization as indicated by a decrease in the number of PCs (Fig. 4A). Similar results were achieved with correlated cortical input to the STN (Fig. 4B). In contrast, cortical inputs impacted synchronization when numerous GJs were present. When cortical input was uncorrelated, higher GJC conductances in the sparse architecture led to partial synchronization, generating a minimum of 4 PCs (Fig. 4C). Under the influence of correlated cortical input, a minimum of 2 PCs could be achieved, indicating almost complete synchronization (Fig. 4D). Thus, in our computational model, synchrony in the basal ganglia depended on pallidal GJC as well as the cortical input to STN. Although the STN itself did not contain any GJs, pallidal GJs could influence its synchrony. Furthermore, reducing the number of GJs to on average 0.25 per cell led to desynchronization at medium GJ conductances (data not shown).

Discussion and Conclusions

We detected Cx36 in the human putamen, GPe, and GPi, suggesting GJC in these nuclei. In contrast, no

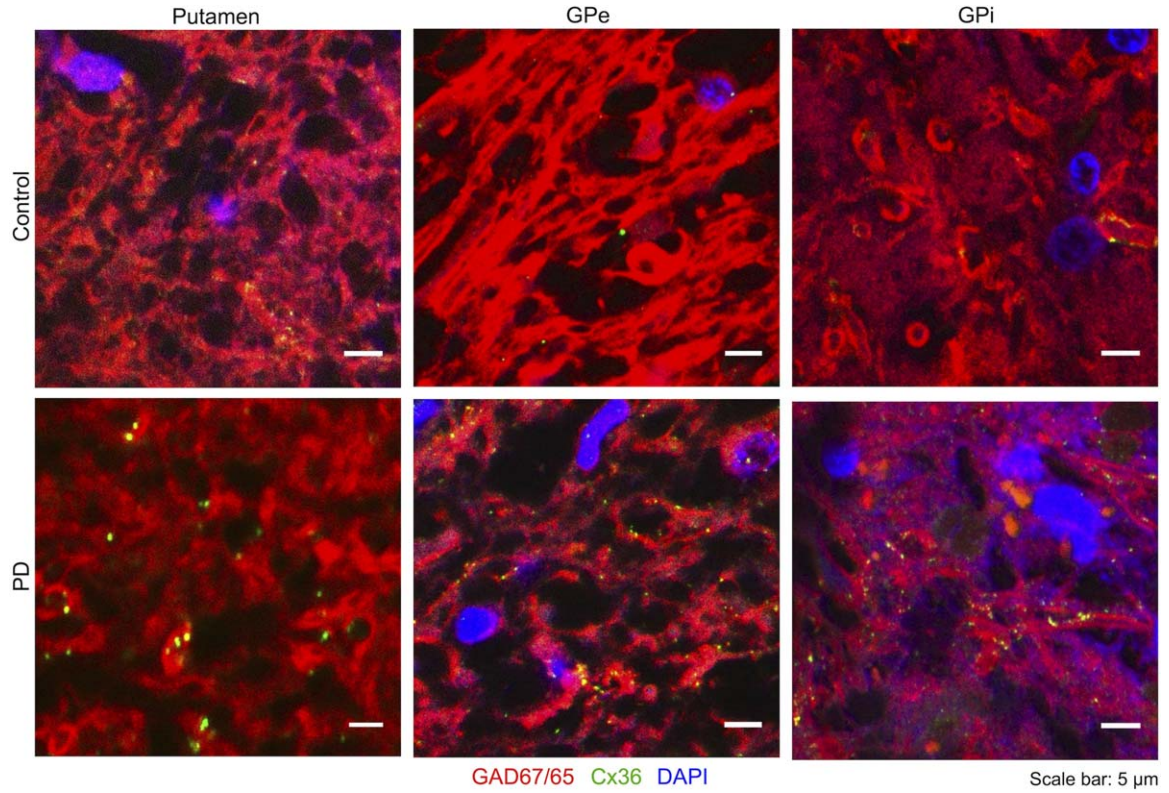

FIG. 2. Cx36 in the human basal ganglia: Small high-resolution outtakes from confocal images. Cell nuclei are labelled by DAPI (blue), GABAergic neurons by anti-GAD65/67 (red) and Cx36 by anti-Cx36 (green). Some Cx36 is present in the putamen, GPe and GPi of control subjects, while an increase of Cx36 can be seen in the PD patients. [Color figure can be viewed in the online issue, which is available at wileyonlinelibrary.com.]

Cx36 was found in the human STN. A Cx36 remodeling was seen in the GPe and GPi of the PD patients. In a small network model of the basal ganglia, we demonstrated that numerous high-conductance GJs rendered the GPe more susceptible to synchronize with cortical inputs transmitted via the STN. Cells of the STN also showed synchrony dependent on pallidal GJs, although they were not coupled via GJs themselves. We suggest pallidal GJC as a mechanism for the transmission and reinforcement of neural synchrony in the dopamine-depleted basal ganglia, which can be tested in vivo or in vitro in an animal model of PD. We predict that the application of a GJ blocker directly on the GPe and GPi will decrease neural synchronization in the dopamine-depleted basal ganglia. Should this prove true, seeing how GJ blocking affects the motor signs of the animal would be interesting. A direct involvement of GJC in the pathophysiology of PD would open up novel treatment possibilities, including pharmacological modulation of GJs.

Our findings of Cx36 in the human GPe and GPi are novel. Cx36 has already been detected in healthy rat

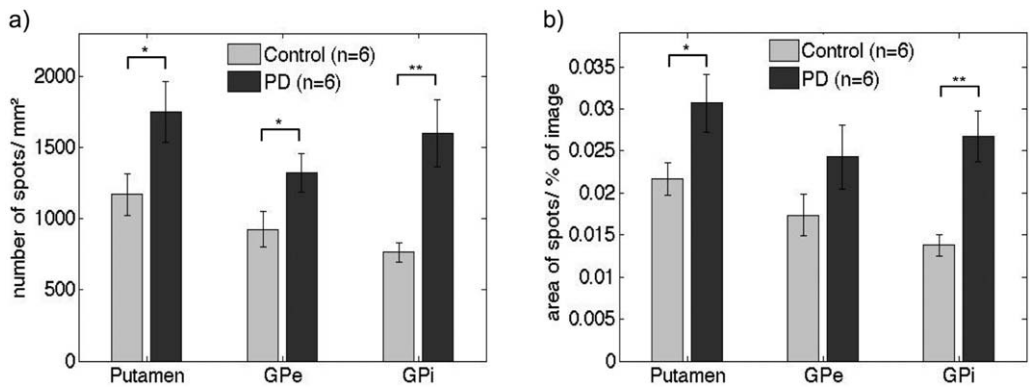

FIG. 3. Average expression of Cx36: (a) number of spots per mm^2; (b) total area of the spots as a fraction of the total image. Cx36 spots are significantly ($p < 0.05$) increased in all three nuclei. The increase in cumulative area of detected Cx36 spots is significant only in putamen and GPi. The standard errors of the mean are presented as thin bars. *$p < 0.05$; **$p < 0.01$ (two sample t-test).

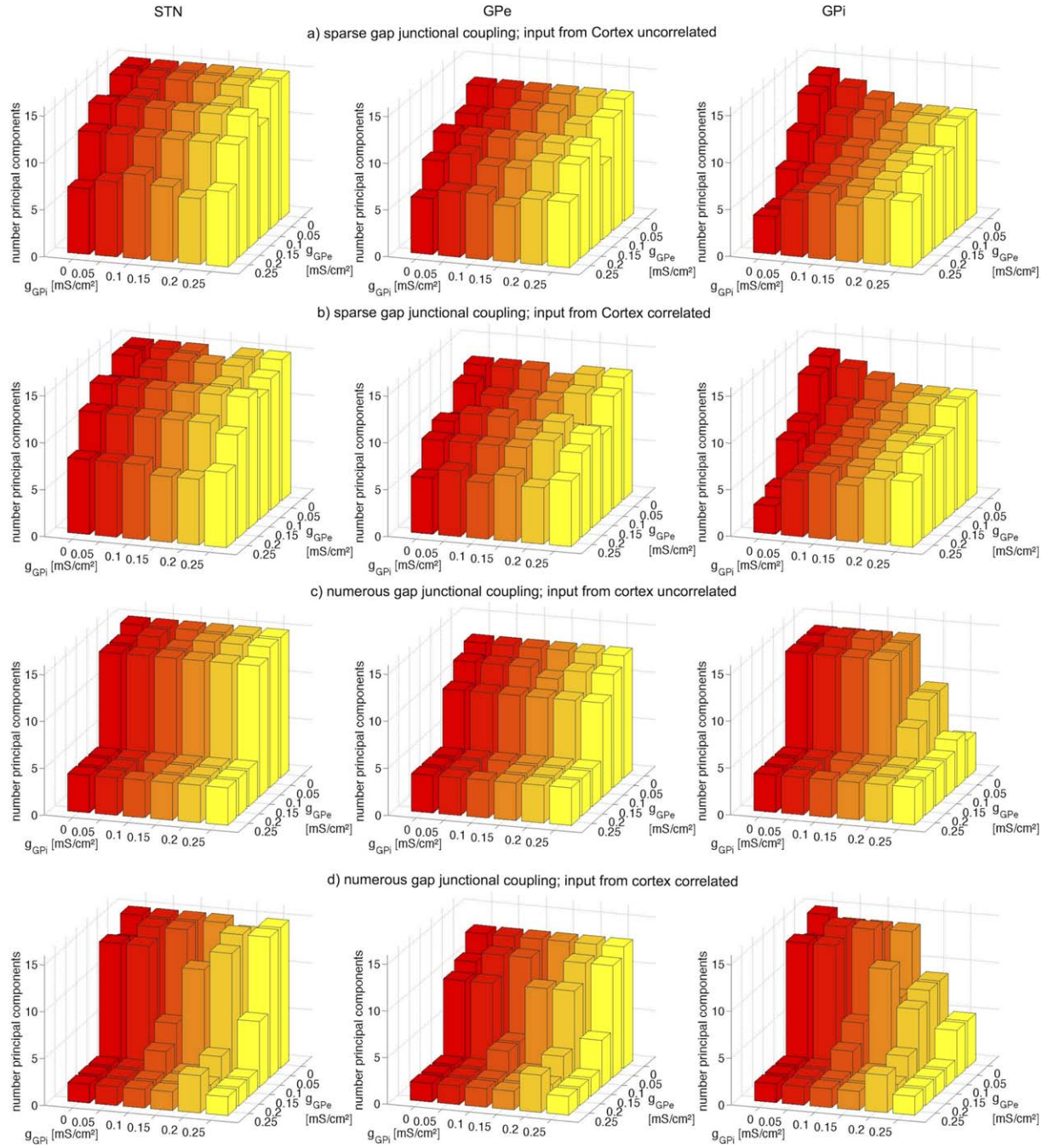

FIG. 4. Results of the computational model. Principal component analysis of neural activity in the STN (first column), GPe (second column) and GPi (third column) at sparse (a and b) and numerous (c and d) GJC in GPe and GPi as well as with uncorrelated (a and c) and uncorrelated (b and d) inputs from the cortex. Bars show the number of principal components dependent on GJ conductance in the GPe (g_{GPe}) and in the GPi (g_{GPi}). Points with GJ conductance zero indicate the reference without GJC. If GJC is sparse, a rise of GJ conductance leads to only moderate synchronization. Correlated input from the cortex is not able to completely synchronize activity in the basal ganglia (a and b). However, if GJC is numerous, the basal ganglia are vulnerable to synchronize with increased gap junction conductances and also with correlated input from the cortex (c and d). [Color figure can be viewed in the online issue, which is available at wileyonlinelibrary.com.]

GP.[27] As with our human tissue, the level of Cx36 in the rat GP was low compared with Cx36 in the rat striatum. Kita[48] also described single GJs in the rat GP using electron microscopy. Although the messenger ribonucleic acid of Cx36 has been found in rat STN and GP,[49] no GJs were found in the rat STN using electron microscopy.[50] We also did not find significant levels of Cx36 in the human STN. Gao et al.[51] showed up-regulated expression of Cx36 in the motor cortex and striatum of a rat model of PD. In the striatum, they found an increase of 38% using immunohistochemistry and 15% with immunoblotting. Similarly, our immunohistochemistry of the putamen yielded a 50% increase in the number of Cx36 spots and a 42% increase in their area.

The use of human tissue imposed limitations on our study. First, the total number of subjects was low, but

all of them showed Cx36 in GPe and GPi. Furthermore, the tissue had postmortem delays between 3 and 8 hours. Although this is a short time for processing human tissue, some proteins may have already degenerated. Moreover, the tissue has been fixed in formalin, which restricts the labeling quality and hinders the possibility of immunoblotting. The quality of the human tissue is therefore not comparable to directly fixed animal tissue. Additionally, most PD patients in this study were treated with L-3,4-dihydroxyphenylalanine (L-dopa), which also may have effects on Cx36 expression. However, PD patients # 7 and # 11 did not receive L-dopa the year before their death, and their Cx36 levels were not lower than those of the other PD patients. In general, postmortem studies do not allow a definite statement on whether the observed changes are causal, compensatory, or epiphenomenal for pathology. Studies with animal models of PD will be appropriate to address these questions in further detail.

We also considered limitations related to GJ functionality and their role in the basal ganglia. First, detection of Cx36 on cell membranes does not directly imply GJC, but also can indicate hemi-channels or nonfunctional GJs. Fukuda et al.[52] estimated that 2% to 5% of Cx36 spots indicate functional GJs in the open configuration. In pathological states such as PD, the average function of the GJs may change. Nevertheless, the occurrence and the detected levels of Cx36 give indications of GJC. We neglected potential GJC between different nuclei, because GJs typically occur between adjacent cells[53] of the same type.[54-57] However, we cannot exclude the possibility of GJC, for example, to and from the striatum, because GJC between different nuclei is potentially not explored yet. Second, we did not investigate the expression of Cxs other than Cx36. GJC between GABAergic neurons mainly involves Cx36,[23,52,58] but in particular glutamatergic neurons may express other Cxs such as Cx45.[59] Thus, we cannot provide a definite statement on the absence of GJs in the human STN. Third, for GJC to occur, we need to assume that anatomical contacts exist between cells. Although local axon collaterals are extensively present in the human GPe,[60] they seem to be low in number in the GPi.[61] Finally, the computational model demonstrated synchronizing roles of pallidal GJs depending on their strength and architecture, but may not realistically reproduce the neural dynamics in the whole basal ganglia. Specifically, it cannot replicate oscillations within different frequency ranges. To achieve this, the model would need to include more cells and account for heterogeneity within the nuclei.

Based on our findings of Cx36 in the human GPe and GPi, we hypothesize GJC in these nuclei. Furthermore, we suggest a remodeling of GJs after neural injury and an increase of GJ conductance after dopamine depletion in PD. In PD patients, dopamine loss also occurs in the GPe (−82%) and GPi (−51%).[62] Application of dopamine to the GP of rat models of PD improved the rats' motor behavior.[63] Dye-coupling in the striatum of 6-hydroxydopamine rat models of PD, indicative of GJC, can increase up to fourfold.[36] A similar increase in GJC in the GPe and GPi after dopamine depletion would be sufficient to trigger synchronization in the basal ganglia. In our computational model, small changes in GJ conductance of approximately 0.05 mS/cm^2 could shift the basal ganglia to a synchronized state. We stress that the pathology of PD also may involve altered GJC in the cortex, striatum, substantia nigra, and retina. Using a computational model, Damodaran et al. [24] described how altered GJC between fast-spiking interneurons of the striatum can lead to an imbalance of the direct and indirect pathways in PD. GJs in the cortex could be involved in the generation of β oscillations.[64] Modulation of the GJs between dopaminergic cells of the substantia nigra pars compacta[65] may contribute to cell death,[66] and similar processes may occur in the retina.

Gap junction remodeling also may depend on factors other than neural injury and the dopamine level. Palacios-Prado et al.[67] demonstrated an increase in GJC with decreasing intracellular magnesium concentration. Given that the intracellular magnesium concentration is decreased in the resting brain of patients with PD and other neurological diseases,[68] GJC may indeed increase in PD. In contrast, Sung et al.[66] showed that overexpression of α-synuclein, as seen in PD brains, can decrease GJC. The role of GJs in health and disease is far from understood, and their interplay with chemical synapses can sculpt neural network dynamics in various ways. ■

Acknowledgment: We thank the Netherlands Brain Bank for providing human tissue and related support, Dr. Anne- Marie van Cappellen van Walsum for help in identifying different brain nuclei, and Dr. Gerco Hassink for his invaluable technical support.

References

1. Wichmann T. Basal ganglia discharge abnormalities in Parkinson's disease. Parkinson's Dis Rel Disord 2006;21-25. http://link.springer.com/chapter/10.1007/978-3-211-45295-0_5.
2. Quiroga-Varela A, Walters JA, Brazhnik E, Marin C, Obeso JA. What basal ganglia changes underlie the parkinsonian state? The significance of neuronal oscillatory activity. Neurobiol Dis, 2013, doi: 10.1016/j.nbd.2013.05.010.
3. Plenz D, Kital ST. A basal ganglia pacemaker formed by the subthalamic nucleus and external globus pallidus. Nature 1999;400:677-682.
4. Terman D, Rubin JE, Yew AC, Wilson CY. Activity patterns in a model for the subthalamopallidal network of the basal ganglia, J Neurosci 2002;22:2963-2976.
5. Bevan MD, Magill PJ, Terman D, Bolam JP, Wilson CJ. Move to the rhythm: oscillations in the subthalamic nucleus-external globus pallidus network. Trends Neurosci 2002;25:525-531.
6. Fan KY, Baufreton J, Surmeier JD, Chan CS, Bevan MD. Proliferation of external globus pallidus-subthalamic nucleus synapses following degeneration of midbrain dopamine neurons. J Neurosci 2013;32:13718-13728.

7. Magill PJ, Bolam JP, Bevan MD. 2001. Dopamine regulates the impact of the cerebral cortex on the subthalamic nucleus–globus pallidus network. Neuroscience 2001;106:313-330.
8. Brown P. Oscillatory nature of human basal ganglia activity: relationship to the pathophysiology of Parkinson's disease. Mov Disord 2003;18:357-363.
9. Sharott A, Magill PJ, Harnack D, Kupsch A, Meissner W, Brown P. Dopamine depletion increases the power and coherence of f3-oscillations in the cerebral cortex and subthalamic nucleus of the awake rat. Eur J Neurosci 2005;21:1413-1422.
10. Hahn PJ, McIntyre CC. Modeling shifts in the rate and pattern of subthalamopallidal network activity during deep brain stimulation. J Comput Neurosci 2010;28:425-441.
11. Tachibana Y, Iwamuro H, Kita H, Takada M, Nambu A. Subthalamo-pallidal interactions underlying parkinsonian neuronal oscillations in the primate basal ganglia. Eur J Neurosci 2011;34:1470-1484.
12. Chan CS, Glajch KE, Gertler TS, et al. 2011. HCN channelopathy in external globus pallidus neurons in models of Parkinson's disease. Nat Neurosci 2011;14:85-92.
13. Miguelez C, Morin S, Martinez A, Goillandeau M, Bezard E, Bioulac B, Baufreton J. Altered pallido-pallidal synaptic transmission leads to aberrant firing of globus pallidus neurons in a rat model of Parkinson's disease. J Physiol 2012;590:5861-5875.
14. Wilson CJ. Active decorrelation in the basal ganglia. Neuroscience 2013;250:467-482.
15. Schwab BC, Heida T, Zhao Y, Marani E, van Gils SA, van Wezel RJA. Synchrony in Parkinson's disease: importance of intrinsic properties of the external pallidal segment. Front Syst Neurosci 2013;7:60.
16. Nini A, Feingold A, Slovin H, Bergman H. Neurons in the globus pallidus do not show correlated activity in the normal monkey, but phase-locked oscillations appear in the MPTP model of parkinsonism. J Neurophysiol 1995;74:1800-1805.
17. Bar-Gad I, Heimer G, Ritov Y, Bergman H. Functional correlations between neighboring neurons in the primate globus pallidus are weak or nonexistent. J Neurosci 2003;23:4012-4016.
18. Raz A, Vaadia E, Bergman H. Firing patterns and correlations of spontaneous discharge of pallidal neurons in the normal and the tremulous 1-methyl-4-phenyl-1, 2, 3, 6-tetrahydropyridine vervet model of parkinsonism. J Neurosci 2000;20:8559-8571.
19. Heimer G, Bar-Gad I, Goldberg JA, Bergman H. Dopamine replacement therapy reverses abnormal synchronization of pallidal neurons in the 1-methyl-4-phenyl-1,2,3,6- tetrahydropyridine primate model of parkinsonism. J Neurosci 2002;22:7850-7855.
20. Yamawaki N, Stanford IM, Hall SD, Woodhall GL. Pharmacologically induced and stimulus evoked rhythmic neuronal oscillatory activity in the primary motor cortex in vitro. Neuroscience 2008; 151:386-395.
21. Traub RD, Whittington MA. *Cortical Oscillations in Health and Disease*. Oxford University Press, 2010.
22. Weinberger M, Dostrovsky JO. A basis for the pathological oscillations in basal ganglia: the crucial role of dopamine. Neuroreport 2011;22:151.
23. Dere E. *Gap Junctions in the Brain*. Elsevier, 2012.
24. Damodaran S, Evans RC, Blackwell KT. Synchronized firing of fast-spiking interneurons is critical to maintain balanced firing between direct and indirect pathway neurons of the striatum, J Neurophysiol 2014;111:836-848.
25. Galarreta M, Hestrin S. Electrical synapses between GABA-releasing interneurons. Nat Rev Neurosci 2001;2:425-433.
26. Fukuda T. Network architecture of gap junction-coupled neuronal linkage in the striatum. J Neurosci 29:1235-1243.
27. Rash JE, Staines WA, Yasumura T, Patel D, Furman CS, Stelmack GL, Nagy JI. Immunogold evidence that neuronal gap junctions in adult rat brain and spinal cord contain connexin-36 but not connexin-32 or connexin-43. Proc Natl Acad Sci U S A 2000;97: 7573-7578.
28. Nemani VM, Binder DK. Emerging role of gap junctions in epilepsy. Histol Histopathol 2005;20: 253-259.
29. Wang Y, Denisova JV, Kang KS, Fontes JD, Zhu BT; Belousov AB. Neuronal gap junctions are required for NMDA receptor-mediated excitotoxicity: implications in ischemic stroke. J Neurophysiol 2010;104:3551-3556.
30. Bargiotas P, Muhammad S, Rahman M, et al. Connexin 36 promotes cortical spreading depolarization and ischemic brain damage. Brain Res 2012;1479:80-85.
31. Belousov AB. Novel model for the mechanisms of glutamate-dependent excitotoxicity: role of neuronal gap junctions. Brain Res 2012;1487:123-130.
32. Fernandez-Suarez D, Celorrio M, Lanciego JL, Franco R, Aymerich MS. Loss of parvalbumin-positive neurons from the globus pallidus in animal models of Parkinson disease. J Neuropathol Exp Neurol 2012;71:973-982.
33. McHahon DG, Knapp AG, Dowling JE. Horizontal cell gap junctions: single-channel conductance and modulation by dopamine. Proc Natl Acad Sci U S A 1989;86:7639-7643.
34. Hampson ECGM, Weiler R, Vaney DI. Regulation of gap-junction permeability between A-type horizontal cells in rabbit retina-effects of ph and dopamine. Invest Ophthalmol 1992;33:1406-1406.
35. Li H, Zhang Z, Blackburn MR, Wang SW, Ribelayga CP, O'Brien J. Adenosine and dopamine receptors coregulate photoreceptor coupling via gap junction phosphorylation in mouse retina. J Neurosci 2013;33:3135-3150.
36. Cepeda C, Walsh JP, Hull CD, Howard SG, Buchwald NA, Levine MS. Dye-coupling in the neostriatum of the rat: I. Modulation by dopamine-depleting lesions. Synapse 1989;4:229-237.
37. Onn SP, Grace AA. Alterations in electrophysiological activity and dye coupling of striatal spiny and aspiny neurons in dopamine-denervated rat striatum recorded in vivo. Synapse 1999;33:1-15.
38. Moore H, Grace AA. A role for electrotonic coupling in the striatum in the expression of dopamine receptor-mediated stereotypies. Neuropsychopharmacology 2002;27:980-992.
39. Rasband WS. Image J. Bethesda, MD: U.S. National Institutes of Health. Available from: http://imagej.nih.gov/ij/.
40. Chow CC, Kopell N. Dynamics of spiking neurons with electrical coupling. Neural Comput 2000;12:1643-1678.
41. Lewis TJ, Rinzel J. Dynamics of spiking neurons connected by both inhibitory and electrical coupling. J Comput Neurosci 2003; 14:283-309.
42. Vervaeke K, Lorincz A, Gleeson P, Farinella M, Nusser Z, Silver RA. Rapid desynchronization of an electrically coupled interneuron network with sparse excitatory synaptic input. Neuron 2010;67:435-451.
43. Pfeuty B. The combined effects of inhibitory and electrical synapses in synchrony. Neural Comput 2005;17:633-670.
44. Rubin JE, Terman D. High frequency stimulation of the subthalamic nucleus eliminates pathological thalamic rhythmicity in a computational model. J Comput Neurosci 2004;16:211-235.
45. MATLAB version 7.14. Natick, Massachusetts, USA: The MathWorks Inc., 2012.
46. Fortier PA. Detecting and estimating rectification of gap junction conductance based on simulations of dual-cell recordings from a pair and a network of coupled cells. J Theor Biol 2010;265:104-114.
47. Lourens MAJ. Neural network dynamics in Parkinson's disease. University of Twente, 2013.
48. Kita H. Parvalbumin-immunopositive neurons in rat globus pallidus: a light and electron microscopic study. Brain Res 1994;657: 31-41.
49. Vandecasteele M, Deniau JM, Glowinski J, Venance L. Electrical synapses in basal ganglia. Rev Neurosci 2007;18:15-36.
50. Chang HT, Kita H, Kitai ST. The fine structure of the rat subthalamic nucleus: an electron microscopic study. J Comp Neurol 1983;221:113-123.
51. Gao M, Wang HL, Wang LC, Chen XW. Modulation of connexin 36 expression in basal ganglia and motor cortex in rat model of Parkinson's disease. Chinese Journal of Contemporary Neurology and Neurosurgery 2013;13:697-703.
52. Fukuda T, Kosaka T, Singer W, Galuske RA. Gap junctions among dendrites of cortical GABAergic neurons establish a dense and widespread intercolumnar network. J Neurosci 2006;26:3434-3443.

53. Soehl G, Maxeiner S, Willecke K. Expression and functions of neuronal gap junctions. Nat Rev Neurosci 2005;6:191-200.

54. Galarreta M, Hestrin S. A network of fast-spiking cells in the neocortex connected by electrical synapses. Nature 1999;402:72-75.

55. Gibson JR, Beierlein M; Connors BW. Two networks of electrically coupled inhibitory neurons in neocortex. Nature 1999;402: 75-79.

56. Tamas G, Buhl EH, Lorincz A, Somogyi P. Proximally targeted GABAergic synapses and gap junctions synchronize cortical interneurons. Nat Neurosci 2000;3:366-371.

57. Hestrin S, Galarreta M. Electrical synapses define networks of neocortical GABAergic neurons. Trends Neurosci 2005;28:304-309.

58. Connors BW, Long MA. Electrical synapses in the mammalian brain. Annu Rev Neurosci 2004;27:393-418.

59. Ma Y, Hioki H, Konno M, et al. Expression of gap junction protein connexin36 in multiple subtypes of GABAergic neurons in adult rat somatosensory cortex. Cerebral Cortex 2011;21:2639-2649.

60. François C, Percheron G, Yelnik J, Heyner S. A Golgi analysis of the primate globus pallidus. I. Inconstant processes of large neurons, other neuronal types, and afferent axons. J Comp Neurol 1984;227:182-199.

61. Parent M, Parent A. The pallidofugal motor fiber system in primates. Parkinsonism Rel Disord 2004;10:203-211.

62. Rajput AH, Sitte HH, Rajput A, Fenton ME, Pifl C, Hornykiewicz O. Globus pallidus dopamine and Parkinson motor subtypes. Neurology 2008;70:1403-1410.

63. Galvan A, Floran B, Erlij D, Aceves J. Intrapallidal dopamine restores motor deficits induced by 6-hydroxydopamine in the rat. J Neural Transm 2001;108:153-166.

64. Traub RD, Bibbig A, Fisahn A, LeBeau FE, Whittington MA, Buhl EH. A model of gamma frequency network oscillations induced in the rat CA3 region by carbachol in vitro. Eur J Neurosci 2000;12: 4093-4106.

65. Vandecasteele M, Glowinski J, Venance L. Electrical synapses between dopaminergic neurons of the substantia nigra pars compacta. J Neurosc 2005;25:291-298.

66. Sung JY, Lee HJ, Jeong EI, Oh Y, Park J, Kang KS, Chung KC. Alpha-synuclein overexpression reduces gap junctional intercellular communication in dopaminergic neuroblastoma cells. Neurosci Lett 2007;416:289-293.

67. Palacios-Prado N, Hoge G, Marandykina A, et al. Intracellular magnesium-dependent modulation of gap junction channels formed by neuronal connexin36. J Neurosci 2013;33:4741-4753.

68. Barbiroli B, Iotti S, Cortelli P, Martinelli P, Lodi R, Carelli V, Montagna P. Low brain intracellular free magnesium in mitochondrial cytopathies. J Cereb Blood Flow Metabol 1999;19:528-532.